WESTERN PACIFIC EARTH SCIENCES
Vol.3, No.2, P.119-132, 5 Figs., 1 Tab., December, 2003

QUATERNARY OCEANOGRAPHIC CHANGES, BASED ON THE DIATOM FOSSIL RECORD IN THE PISTON CORE MD972144 IN THE SOUTH CHINA SEA

JING-MIIN LIN[1], WEI-LUNG WANG[1,*], LIANG-CHI WANG[1], MENG-YANG LEE[2], TEH-QUEI LEE[3] AND KUO-YEN WEI[2]

1. Department of Biology, National Changhua University of Education, Changhua, Taiwan
2. Department of Geosciences, National Taiwan University, Taipei, Taiwan
3. Institute of Earth Sciences, Academia Sinica, Taipei, Taiwan
* Corresponding author E-mail: wlwang@cc.ncue.edu.tw

ABSTRACT

The core MD972144 (19°36'N, 120°53'E) recovered from the South China Sea was used for establishing the changes of diatom and its abundance which based on its taxonomy and morphology. A total of 245 diatom taxa were identified throughout the core. Among them, *Chaetoceros* spp., *Thalassionema nitzschioides* and *Thalassiothrix longissima* were the common taxa and their relative abundance ranged from 5% to 70%. The average of diatom abundance was estimated at 3.8×10^7 cells/g DW. The result of Q-mode factor analysis showed that factor 1 was composed mainly of *Thalassionema nitzschioides* and *Thalassiothrix longissima*. The former had the highest factor score (12.486) and predominated during the oxygen isotopic stages late 7, 5, 3, and 1. The diatom temperature index (Td index) was also the highest in these stages. The latter showed the extreme negative score, -12.533, and dominated at the stages 6, 4, and 2. Factor 1 generally reflected the temperature signal of the water masses. In addition, the diatom assemblage of this core during the glacial periods was characterized by a low in the Td index and relative abundance of the characteristic species of the Kuroshio Current and upwelling indicators and corresponded to a declining marine environment. Conversely, all the above indicators showed opposite characteristics during the interglacial periods.

Key words: fossil diatom, South China Sea, Kuroshio Current, Td index, Quaternary

INTRODUCTION

The South China Sea is characterized by high resolution rates and excellent fossil preservation in the Western Pacific Warm Pool (Wang and Wang, 1990; Miao *et al.*, 1994) and located between the East Asian landmass and the western Pacific, which makes this marginal sea very sensitive to climate changes, especially to the monsoon system. It has broad shelves in the northern and southwestern regions, while in the middle and eastern parts are deep-sea basins, with an average depth of *ca.* 4000 m. The carbonate compensation depth of the South China Sea is about 3500 m.

The South China Sea is strongly influenced by the East Asian Monsoon system. The circulation of surface water is mainly driven by the annually reversing monsoon winds which create large volumetric changes in the surface water flow. At present, the warm Indian Ocean surface water flows through the shallow Sunda Shelf into the southern South China Sea during the summer, when the southwest monsoon prevails. The sea surface temperature of the South China Sea is quite uniformly distributed in summer, ranging from 28°C to 29°C. The summer monsoon is characterized by high rainfalls which result in low surface salinities in the region. The average salinity of summer sea surface in this region ranges from 32.8 to 33.6‰. In contrast, the northeast monsoon prevails during the winter. Colder waters from the north flow into the South China Sea through the Taiwan Strait, while a branch of the warm Kuroshio Current enters the South China Sea through the Luzon Strait (Shaw, 1991). These two surface water masses combine and flow southward along the coast of Asia, and form a counterclockwise gyre in the South China Sea. The inflow of northern water into the South China Sea results in a large temperature gradient between the northern and southern parts of the South China Sea. The temperature of the sea surface ranges from *ca.* 18°C in the north to *ca.* 27°C in the south, and the salinity of the sea surface ranges from 33.2 to 34.4‰.

The South China Sea was a semi-enclosed marginal sea during the last glacial period. The sea level was *ca.* 120 m lower than present (Fairbanks, 1989) and was connected to the western Pacific Ocean through the Luzon Strait, and to the Sulu Sea through the Balabac and Mindoro Straits. The warm water from the Indian Ocean was cut off by the emergence of the Sunda Shelf (Wang and Wang, 1990).

The sedimentation rate in the South China Sea is higher than those in other parts of the Pacific Ocean. Foraminifera fossils have been used to reconstruct the paleoenvironment (Wang and Wang, 1990; Miao *et al.*, 1994; Huang *et al.*, 1997a, b). Based on the microfossils, the changes in monsoon and surface currents between the glacial and the interglacial periods might be better explained. Diatom fossil research in this area is rare, however, it is also a very important way to reconstruct the paleoclimate and to test the different hypothesis in the past South China Sea. In core MD972144, we tried to use diatom assemblages, Td index and Q-mode factor analysis to presume the characteristics of the paleoceanography in the South China Sea.

MATERIAL AND METHODS

Modern oceanographic setting

The South China Sea is one of the largest marginal seas surrounded by the Pacific Ocean and the India Ocean. It is a tropical region possessed both the characteristics of a terrigenous marginal sea and a half-closed basin. The Taiwan Strait, the Luzon Strait, the Mindoro Strait, the Balabac Strait, the Karimata Strait and the Malacca Strait are the channels for the South China Sea to connect with the Pacific Ocean, the Sulu Sea, the Java Sea, and the India Ocean, respectively (Morton and Blackmore, 2001). The depths of those channels are not deeper than 500 meters, except the Luzon Strait (depth of 2200 meters). The surface water could be connected to the India Ocean and the Pacific Ocean through the Sunda Shelf and the Luson Strait, respectively. The Luzon Strait is the only way for the exchange of deep and intermediate water masses between the marginal seas and the ocean.

In the late glacial period, the South China Sea was very distinct in showing that the sea level was depressed about 120 meters (Fabirbanks, 1990), and 1/5 of the reefs was exposed. The surface currents only flowed in through the 2200 m deep Luzon Strait at the northest and formed as a semi-closed basin (Wang and Wang, 1990). The surface current circulation, SST, wind-dependant upwelling, biological production, and the flux of terrigenous materials are all influenced seasonally by the East Asia Monsoon. In the interglacial period, the current was clockwise in summer and counterclockwise in winter (Shaw and Chao, 1994). The surface water was low in salinity and high in temperature in summer because the southwest monsoon intensified the precipitation. However, the northeast monsoon accelerated a favorable water mass exchange and induced the intrusion of the Kuroshio Current in the north of Luzon Island from September to April (Shaw and Chao, 1994). The winter monsoon played an important role in the SST and biological productivity (Wang and Wang, 1990; Hung *et al.*, 1997a; Chen and Huang, 1998).

Lithology and age model of core MD972144

Core MD972144 was retrieved from the northwest of Luzon Island in the South China Sea during the IMAGES III cruise in 1997 (Fig. 1). It has a total recovered length of about 35. 3 m and mainly consisted of dark olive-gray hemipelagic mud with a massive structure, except for many tephra. An age model for this core was constructed based on the oxygen isotope chronology (Fig. 2). The bottom of this core has an age of about 200 kyr, i.e. stage 7a. The sedimentation rate is estimated to be of about 16 cm kyr^{-1} on average.

Microscopic examination

For quantitative analysis, 0.5 gram of dry sediment was subsampled and chemically treated to clean and concentrate the diatoms. The calcium carbonate component was removed by adding concentrated HCl (10%), and the organic matter was oxidized using hydrogen peroxide (H_2O_2, 30%). Fractions were diluted in 20ml of distilled water which were pipetted onto a glass slide, using Pleurax as the mounting medium. Light-microscopic observations were made at magnifications of 1000 x, at least 400 valves were counted per sample, and specific frequencies were computed.

The Td index (the diatom temperature index) method follows Koizumi (1989). Q-mode factor analysis was carried out to summarize the specific temporal variation. Seventeen species having more than 1% frequency were selected as variances then referring to the spatial distribution of diatom thanatocoenoses reported in the South China Sea, various environmental factors were determined. Statistical operations were performed with MiniTab statistic software (Minitab Inc, R.13).

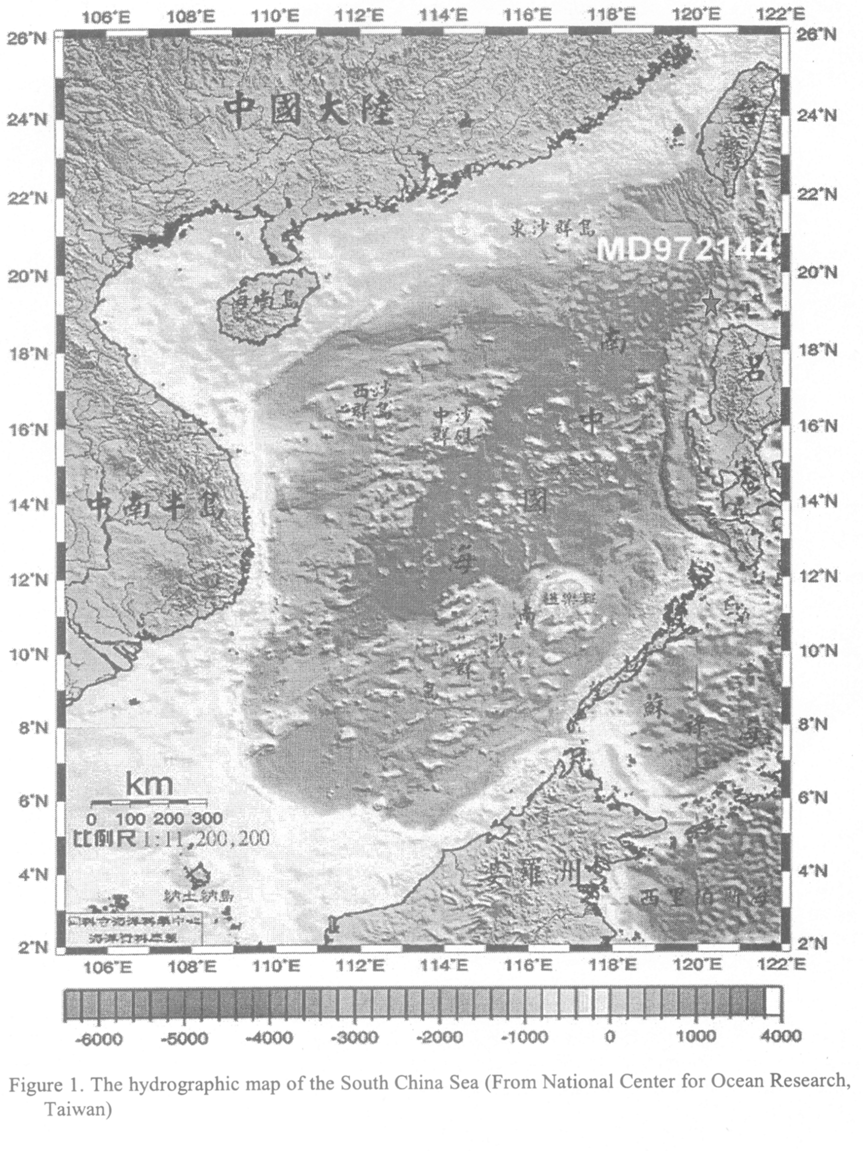

Figure 1. The hydrographic map of the South China Sea (From National Center for Ocean Research, Taiwan)

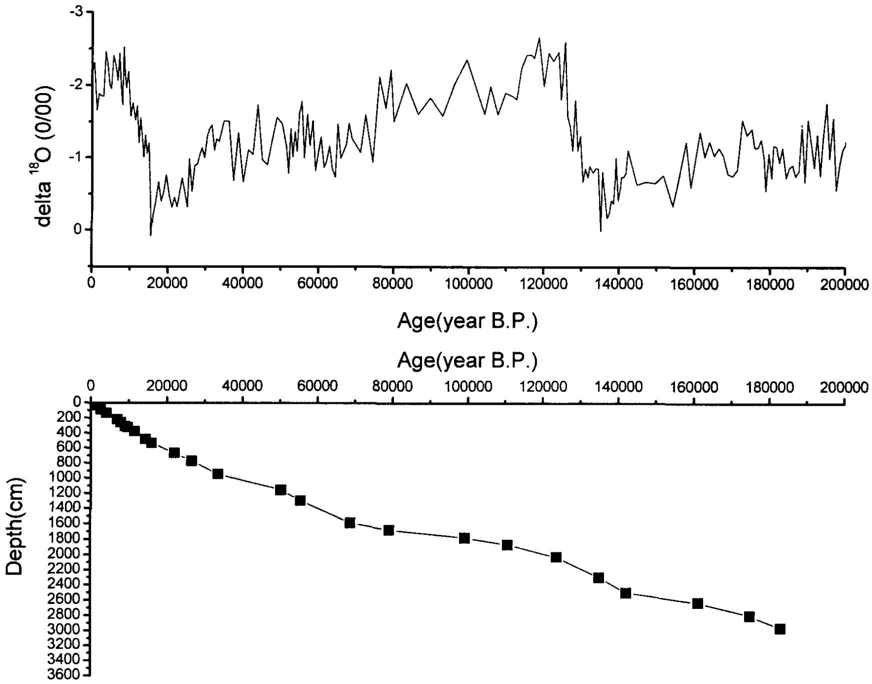

Figure 2. Age model based on the $\delta^{18}O$ stratigraphy of core MD972144.

RESULTS

Preservation and frequency distributions of diatoms

Diatoms were well preserved in the deposits during the glacial stages 6, 4, and 2, whereas sediments of the stages 7a, 5, 3, and 1 were nearly barren of undamaged diatoms (Fig. 3). The average of diatom abundance was estimated at about 3.8×10^7 cells/g DW. The strongest peak of abundance was located in late stage 6 (depth of 2271 cm), about 13.7×10^7 cells/g DW, but dropped drastically in the transition from stage 6 to 5 (depth of 2091 cm).

There were 66 genera and 245 species observed throughout this core. The diatom assemblages were mainly composed of tropical-subtropical plankton species. *Chaetoceros* spp., *Thalassionema nithtzschioides*, and *Thalassiothrix longissima* were the most significant species with an abundance of more than 10%. The frequency of *Thalassionema nithtzschioides* averaged 36.6 % throughout the core, and predominated at the stages 7a, 5, 3 and 1 and

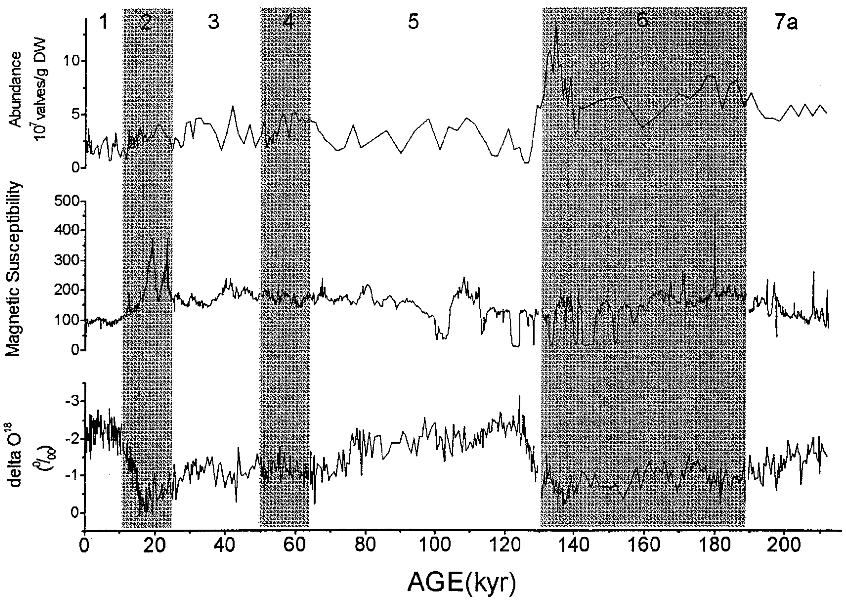

Figure 3. Stratigraphic change of the abundance. This figure shows the correlation of the abundance with the δO^{18} stratigraphy and magnetic susceptibility.

corresponded to the warm periods (Fig. 4). The cold water species, *Thalassiothrix longissima* predominated at stages 6, 4, and 2 and corresponded to the cold periods (Fig. 4). It is well known that the upwelling indicator species, *Chaetoceros* spp., *Paralia sulcata*, *Thalassionema nitzschioides*, and *Thalassiosira lineate* were generally abundant in the open oceans. Besides *Thalassionema nithtzschioides*, there were two apparent peaks of *Chaetoceros* spp. observed in the stages 5 and 1, respectively (Fig. 4) and might imply some significance of upwelling in the area studied. However, the abundance of *Paralia sulcata* and *Thalassiosira lineate* were less than 5%, and did not havesignificant changes throughout the core.

Td index and Q-mode factor analysis

The trend of the Td index was well correlated to that of the oxygen isotope, which showed high in the interglacial period and low in the glacial period (Fig. 5). The Td index oscillated drastically from 0.6 to 0.3 from late stage 7 to stage 6, and rose slightly at stage 5. The clear negative shift occurred at the boundary of the stage 5/4, and rose again at the late stage 4. Subsequently, the trend decreased to the lowest value 0.1 at the depth of 551 cm in stage 2. Other drastic and positive shifts occurred at the boundary of stage 2/1, and the highest value was found at the depth of 171 cm in stage 1 but decreased by late stage 1.

As a result of the Q-mode factor analysis, 2 factors were delineated with a cumulative

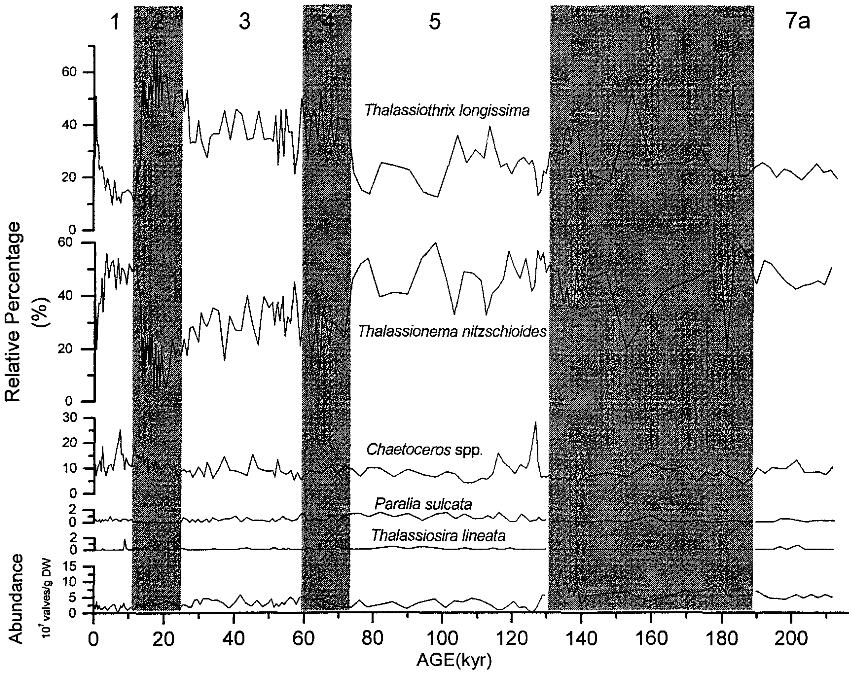

Figure 4. Stratigraphic distribution of frequency of the primary upwelling species.

contribution accounting for 94.8% of the diatom assemblage data (Table 1). Factor 1 (F1) showed factor scores that accounted for 88.5% of all variance consisted mostly of *Thalassionema nitzschioides* and *Thalassiothrix longissima*. *Thalassionema nitzschioides* had the highest factor score (12.486) and dominated at the warm stages of late 7, 5, 3, and 1. However, *Thalassiothrix longissima* showed the extreme negative score, -12.533, and dominated at the cold stages of 6, 4, and 2. The downcore values for varimax factor loading are shown in Fig. 5. Factor 1 loading was high during stages late 7, 5, 3 and 1, the warm period. Thus, F1 reflected the signal of the warm water masses and the factor loading changed and exhibited a high correlation with the Td index value (Fig. 5).

The major component of factor 2 (F2) which showed factor scores accounted for 6.3% of all variance includes *Tn. nitzschiaides*, *Talassiothrix longissima* and *Chaetoceros* spp. (Table 1). *Thalassionema nitzschiaides*, and *Talassiothrix longissima* had higher positive scores 1. 448 and 1.754, respectively (Table 1). *Chaetoceros* spp. had a negative score, -3.422. The trend of F2 factor loading was inopposition to the abundance of coastal species throughout the core. On the whole, we inferred that F2 represented the ratio of the neritic and the oceanic diatom assemblages.

Table 1. List of the factor scores and high-scores species. Varimax rotation was carried out.

Factors	Factor 1	Factor 2
Contribution(%)	88.5	6.3
Cumulative contribution(%)		94.8
Azpeitia nodulifer	-0.1560	-0.1323
Bacteriastrum spp.	-0.0124	0.0518
Chaetoceros spp.	0.0925	**-3.4217**
Ethmodiscus rex	0.0411	-0.0325
Fragilariopsis doliolus	-0.0603	0.0109
freshwater diatoms	-0.2897	0.0487
Nitzschia inturreptestriata	0.1769	-0.0610
Nitzschia marina	0.1399	-0.4048
Nitzschia sicula	-0.0404	0.0639
Rhaphoneis amphiceros	0.0133	0.0322
Rhizosolenia hebetata	0.0003	0.0164
Rhizosolenia sp.	-0.1069	0.0213
Thalassionema nitzschioides	**12.4859**	**1.4483**
Thalassiosira eccentrica	0.0912	0.0871
Thalassiosira oestrupii	0.1125	0.1581
Thalassiothrix longissima	**-12.5333**	**1.7536**
Unknown sp.6	-0.0268	0.0399

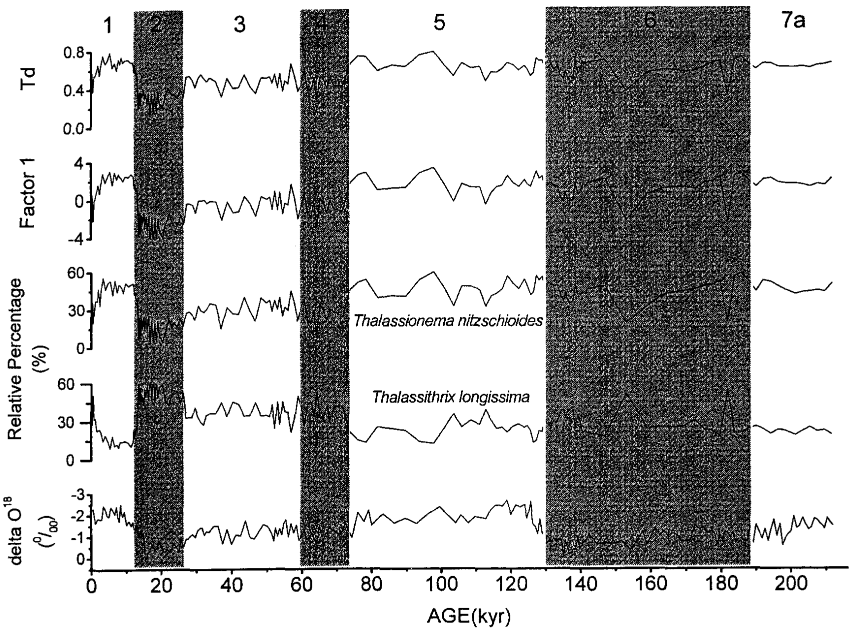

Figure 5. Stratigraphic change of Q-mode factor analysis and Td index, compared to the stratigraphic curve of the δO^{18} and two main diatom species extracted from factor 1.

DISCUSSION

Diatom assemblages and its abundance

The diatom productivity was up to 74% in the modern NE China Sea (Huang, 1993) and suggested that the diatom abundance could be used as the primary productivity indicator in this area. The winter monsoon upwelling prevailed in the South China Sea (Chao *et al.*, 1996; Shaw *et al.*, 1996). In this study area, the upwelling strength was influenced by the winter monsoon and Kuroshio Current. Hence, the diatom abundance could reflect productivity and infer the strength of upwelling.

The diatom abundance could be distinguished into two periods at the boundary of stages 6 and 5. They showed higher abundance than its average at stages 7 and 6, and lower than its average from stage 5 to stage 1 (Fig. 3). We supposed that the result may be formed due to the different diatom cell sizes or the diluting effect by terrigenous material inputs. However, the cell size did not have significant changes in observation of the smear slide throughout the core.

But the magnetic susceptibility (MS) pattern showed high values in the low diatom abundance zones (Fig. 3, Lee, unpublished), which reflected the inputs of the regional terrigenous materials. Thus, the terrigenous input is considered to play a very important role in this core, MD972144. The main sources of the terrigenous material could be from rivers and marine ice abrasion of the surrounding shoreline. We suggested that the diatom abundance was diluted by terrigenous inputs, especially in the glacial period and cannot really reflect the diatom abundance.

Although strong dilution of the terrigenous materials did occur in the study area, the diatom abundance in MD972144 was still 1000 and 100 times than the core KL37 and KL29 in the northern South China Sea and the core KL91 in the southern South China Sea, respectively (Lan *et al.*, 1995). The surface sediment research also supported the conclusion that the diatom abundance was high in the NE South China Sea (Lu, 2001). The high productivity could be inferred to the occurrence of upwelling in this area.

Based on the diatom assemblages and the productivity changes, the marine environment situation could be presumed. *Thalassionema nitzschioides*, the oceanic upwelling indicator (Hasle and Mandiola, 1967; Sancetta, 1979, 1982; Schuette and Schrader, 1981; Sancetta *et al.*, 1992a; Abrantes and Moita, 1999; Shimada and Hasegawa, 2001) had different meanings in different areas. In the Bering Sea, for instance, *Thalassionema nitzschioides* occurred in the sediment by way of the Kuroshio Current pass (Sancetta, 1979), and could be like the Kuroshio Current indicator. Commonly, the occurrence of *Thalassionema nitzschioides* inferred high productivity in the open ocean. The result in this study, however, presented high productivity in the interglacial period and low productivity in the glacial period, which was contrary to previous studies in the NE South China Sea (Wang *et al.*, 1995; Jian *et al.*, 2001). This evidence suggested that the strength of upwelling was not only controlled by the winter Monsoon, but also the Kuroshio Current. And the latter might be a much important factor (Chao *et al.*, 1996). The Kuroshio Current was reported to move easterly in the glacial periods, because of the exposition of reefs were found (Sawada and Handa, 1998; Ujiie and Ujiie, 1999) and the relative abundance of *Thalassionema nitzschioides* was increased. Such results suggested that *Thalassionema nitzschioides* could be the Kuroshio Current indicator species in this area. Based on this suggestion, the strength of upwelling was considered to be reduced by the easterly Kuroshio Current in the glacial periods, and presented lower productivity than in the interglacial periods.

Chaetoceros spp. appeared at the place where productivity was high, but spores were only preserved in areas where the production of the siliceous organisms was so great and the accumulation of silica in the bottom sediment was high, leading to excellent preservation (Guillard and Kilham, 1977; Sancetta, 1982; Sancetta *et al.*, 1992a; Abrantes, 1988, 2000; Zielinski and Gersonde, 1997; Koning *et al.*, 2001). *Paralia sulcata* is a benthic littoral species but also occurs as plankton in the upwelling zone. Some researchers identified it as an upwelling indicator in the east Pacific littoral area (Sancetta *et al.*, 1992b, Kennington *et al.*, 1999). The relative abundance of *Chaetoceros* spp. and *Paralia sulcata* were both presented high in interglacial periods and low in glacial periods (Fig. 4) as well as the ratiocination of the weak Kuroshio Current.

In brief, although huge terrigenous material diluted the diatom signal, the great productivity inferred the existence of upwelling in the NE South China Sea. The relative abundance of the Kuroshio Current indicator, *Thalassionema nitzschioides*, and the upwelling indicator, *Chaetoceros* spp. and *Paralia sulcata*, demonstrated the event of easterly Kuroshio Current and abated upwelling in the glacial periods.

Use of the Td index and Q-mode factor analysis to reconstruct SST

Td index (relative abundance of warm species *vs.* relative abundance of warm and cold species) is a useful index for paleo-SST reconstruction and usually used in high latitudes, such as the North Pacific and the Arctic regions (Jouse, 1962; Sancetta, 1982; Sancetta and Silvestri, 1986; Barron, 1992). In this study, we used it in low latitudes. First, we used the data reported from the cores of DSDP Site 580 (41°37.47'N, 153°58.58'E) in the NW Pacific Ocean (Barron, 1992) and KH-79-3, L-3 in the south Japan Sea (37°04.3'N, 134°42.2'E) (Koizumi, 1989) to examine the practicability of the Td index. The results show that the Td index values increase gradually from high to low latitudes and the trend is the same as the SST changes in the modern ocean and seems to suggest that Td index is practicable and could be used in the low latitudes. Second, the trend of Td index shows that the glacial and interglacial cycles were similar to those of the oxygen isotope: high values during the interglacial periods and low values during the glacial periods. The result also agreed with the previously reported SST data in the northern South China Sea (Wang and Wang, 1990). Furthermore, the SST changes were suggested to follow the global ice-volume change in the South China Sea because of the decreasing of the winter SST (Miao *et al.*, 1994; Wang and Wang, 1990; Huang *et al.*, 1997b) and the sea-level fall in glacial times were impeded by the China coastal current into the South China Sea (Wang and Wang, 1990; Huang *et al.*, 1997b). The SST was affected mostly by the strength of northeast monsoon in the northern South China Sea (Wang and Wang, 1990). Based on this evidence, we suggested that the Td index value could be presumed for the NE monsoon condition in the area studied. The Td index values of our core showed a decreasing trend after stage 5 and reached the lowest value at stage 2, suggesting the same trend of northeast monsoon strength as reported by the other core samples from the South China Sea (Huang *et al.*, 1997a; Jian *et al.*, 2001) and the records in the China loess (Xiao *et al.*, 1995; Guo *et al.*, 1998). Thus, we suggested the Td index was practicable for the NE South China Sea.

In Q-mode factor analysis, the value of F1 and *Thalassionema nitzschioides*, the warm water mass indicator, was high in the interglacial periods and low in the glacial periods and the same as the Td index value (Fig. 5). The warm pool surface water inflow from the India Ocean and the Pacific Ocean to the South China Sea may be reduced significantly when the sea level fell during the glacial periods. This phenomenon led a great decreasing of SST in the South China Sea rather than in the open ocean of the surrounding area (Chen and Hung, 1998; Chen *et al.*, 1999; Wang *et al.*, 1999) and affected the warm-water indicator ratio. Based on the result of the SST in the interglacial and glacial cycles, the east-moved event of the Kuroshio Current water was induced by the falling sea level. The legitimate strength of the events decreased in the glacial period and increased in the interglacial period. As a result, a more-detailed sediment analysis was necessary, particularly the geochemical parameters and terrigenous input in the north Philippines.

CONCLUSION

We can summarize the paleoceanographic scenario in the northern South China Sea for the last 200 kyr based on the diatom quantitative analysis. The amounts of terrigenous inputs diluted the diatom abundance and cannot reflect the real primary productivity. Based on the relative abundance of the species indicating the upwelling and the Kuroshio Current, high values were found in interglacial times and low in glacial times and effects the variation of the strength of Kuroshio Current and the upwelling of the study area. The result showed relative low productivity in the glacial period more due to the eastward movement of the Kuroshio Current than due to the winter monsoon in the NE South China Sea. In addition, based on the Td index, first used in the low latitudes, the reconstructed paleo-SST was similar to previous studies in the South China Sea. In addition, Q-mode factor analysis pointed out that downcore loading of the factor 1, referred to the warm water mass, was very similar to the Td index. The most reasonable interpretation might be due to that the warm water mass from the India Ocean has been cut off in glacial times when the sea level fell.

ACKNOWLEDGMENTS

This study was supported by National Science Council, Republic of China (NSC 90-2611-M-018-001-IM).

REFERENCES

Abrantes, F. (1988) Diatom productivity peak and increased circulation during latest Quaternary: Alboran Basin (western Mediterranean): *Mar. Micropaleotol.*, **13**, 79-96.

Abrantes, F. (2000) 200,000 yr diatom records from Atlantic upwelling sites reveal maximum productivity during LGM and a shift in phytoplankton community structure at 185,000 yr: *Earth Planet. Sci. Lett.*, **176**, 7-16.

Abrantes, F. and Moita, M.T. (1999) Water column and recent sediment data on diatoms and coccolithophorids, off Portugal, confirm sediment record of upwelling events: *Oceanol. Acta*, **22**, 67-84.

Barron, J.A. (1992) Pliocene paleoclimatic interpretation of DSDP Site 580 (NW Pacific) using diatoms: *Mar. Micropaleontol.*, **20**, 23-44.

Chao, S.Y., Shaw, P.T. and Wu, S.Y. (1996) Deep sea ventilation in the South China Sea: *Deep-Sea Res.*, **43**(4), 445-466.

Chen, M.T. and Huang, C.Y. (1998) Ice-volume forcing of winter monsoon climate in the South China Sea: *Paleoceanogr.*, **13**(6), 622-633.

Chen, M.T., Wang, C.H., Huang, C.Y., Wang, P., Wang, L. and Sarnthein, M. (1999) A late Quaternary planktonic foraminifer faunal record of rapid climatic changes from the South Shina Sea: *Mar. Geol.*, **156**, 85-108.

Fairbanks, R.G. (1990) The age and Origin of the "Younger Dyras Climate Event" in Greenland ice core: *Paleoceanogr.*, **6**, 937-948.

Guillard, R. and Kilham, P. (1977) The ecology of marine planktonic diatoms: In D. Werner Ed., The Biology of Diatoms., University California Press, 372-388.

Guo, Z., Liu, T., Fedoroff, N., Wei, L., Ding, Z., Wu, N., Lu, H., Jiang, W. and An, Z. (1998) Climate extremes in Loess of China coupled with the strength of deep-water formation in the North Atlantic: *Global Planet. Change*, **18**, 113-128.

Hasle, G.R. and Mandiola, B.R. (1967) The fine structure of some *Thalassionema* and *Thalassiothrix* species: *Phycologia*, **6**, 107-125.

Huang, C.Y., Liew, P.M., Meixum, Z., Chang, T.C., Kuo, C.M., Chen, M.T. Wang, C.H. and Zheng, L.F. (1997a) Deep sea and lake records of the southeast Asian paleomonsoons for the last 25 thousand years: *Earth Planet. Sci. Lett.*, **146**, 59-72.

Huang, C.Y., Wu, S.F., Zhao, M., Chen, M.T., Wang, C.H., Tu, X. and Yuan, P.B. (1997b) Surface ocean and monsoon climate variability in the South China Sea since the last glaciation: *Mar. Micropaleontol.*, **32**, 71-94.

Huang, R. (1993) Phytoplankton distribution in the South China Sea and Kuroshi-flowing region of Taiwan: *Acta Oceanogr. Taiwanica*, **31**, 73-82.

Jian, Z., Huang, B., Kuhnt, W. and Lin, H.L. (2001) Late Quaternary upwelling intensity and East Asian monsoon forcing in the South China Sea: *Quat. Res.*, **55**, 363-370.

Jouse, A.P. (1962) Stratigraphic and paleogeographic investigation in the northwest low-salinity part of the Pacific Ocean: Akad. Nauk SSSR, Oceanology Ibst., Moscow, 258pp.

Kennington, K., Haslett, S.K. and Funnell, B.M. (1999) Offshore transport of neritic diatoms as indicators of surface current and trade wind strength in the Plio-Pleistocene eastern equatorial Pacific: *Palaeogeogr., Palaeoclimatol., Palaeoecol.*, **149**(1-4), 171-181.

Koizumi, I. (1989) Holocene pulses of diatom growth in the warm Tsushima Current in the Japan Sea: *Diatom Res.*, **4**, 55-68.

Koning, E., van Iperen, J.M., van Raaphorst, W., Helder, W., Brummer, G.J.A. and van Weering, T.C.E. (2001) Selective preservation of upwelling-indicating diatoms in sediments off Somalia, NW Indian Ocean: *Deep-Sea Res.*, **48**, 2473-2495.

Lan, D.Z., Cheng, Z.D. and Liu, S.C. (1995) Diatoms in late quaternary sediments from the south China Sea: China Ocean Press, 138pp. (in Chinese)

Lu, C. (2001) Diatom distribution in surface sediments in the deep-sea area of the South China Sea: *Mar. Geol., Quat. Geol.*, **21**(2), 27-30. (in Chinese)

Miao, Q., Thunell, R.C. and Andeson, A.M. (1994) Glacial-Holocene carbonate dissolution and sea surface temperatures in the South China and Sulu seas: *Paleoceanogr.*, **9**(2), 269-290.

Morton, B. and Blackmore, G. (2001) Southern China Sea: *Mar. Pollution Bull.*, **42**(12), 1236-1263.

Sancetta, C. (1979) Use of semiquantitative microfossil data for paleoceanography: *Geol.*, **7**, 88-92.

Sancetta, C. (1982) Distribution of diatom species in surface sediments of the Bering and Okhotsk seas: *Micropaleontol.*, **28**(3), 221-257.

Sancetta, C. and Silve, S. (1986) Pliocene-Pleistocene evolution of the North Pacific Ocean-atmosphere system, interpreted form fossil diatoms: *Paleoceanogr.*, **1**, 163-180.

Sancetta, C. Heusser, L. and Hall, M.A. (1992a) Late Pliocene climate in the southeast Atlantic: Preliminary results from a multi-disciplinary study of DSDP Site 532: *Mar. Micropaleontol.*, **20**, 59-75.

Sancetta, C., Lyle, M., Heusser, L., Xahn, R. and Bradbury, J.P. (1992b) Late-glacial to Holocene changes in winds, upwelling, and seasonal production of the northern California Current system: *Quat. Res.*, **38**, 359-370.

Sawada, K. and Handa, N. (1998) Variability of the path of the Kuroshio ocean current over the past 25,000 years: *Nature*, **392**, 592-595.

Schuette, C. and. Schrader, H. (1981) Diatom taphocoenoses in coastal upwelling areas of South West Africa: *Mar. Micropaleontol.*, **6**, 131-155.
Shaw, P.T. (1991) The seasonal variation of the intrusion of the Philippine Sea Water into the South China Sea: *J. Geophys. Res.*, **96**(C1), 821-827.
Shaw, P.T. and Chao, S.Y. (1994) Surface circulation in the South China Sea: *Deep-Sea Res.*, **41**(11/12), 1663-1683.
Shaw, P.T., Chao, S.Y., Liu, K.K., Pai, S.C. and Liu, C.T. (1996) Winter upwelling off Luzon in the northeastern South China Sea: *J. Geophys. Res.*, **101**, 16435-16448.
Shimada, C. and Hasegawa, S. (2001) Paleoceanographic implications of a 90,000 year long diatom record in piston core KH94-3, LM-8 off NE Japan: *Mar. Micropaleontol.*, **41**(3-4), 153-166.
Ujiie, H. and Ujiie, Y. (1999) Late Quaternary course changes of the Kuroshio current in the Ryukyu Arc region, northwestern Pacific Ocean: *Mar. Micropaleontol.*, **37**, 23-40.
Wang, L. and Wang, P. (1990) Late Quaternary paleoceanography of the South China Sea: Glacial-interglacial contrasts in an enclosed basin: *Paleoceanogr.*, **5**(1), 77-90.
Wang, P., Wang, L., Bian, Y. and Jian, Z. (1995) Late Quaternary paleoceanography of the South China Sea: Surface circulation and carbonate cycles: *Mar. Geol.*, **127**, 145-165.
Wang, L., Sarnthein, M., Erlenkeuser, H., Grimalt, J., Grootes, P., Heilig, S., Ivanova, E., Kienast, M., Peljero, C., and Pflaumann, U. (1999) East Asian monsoon climate during the Late Pleistocene: High-resolution sediment records from the South China Sea: *Mar. Geol.*, **156**(1-4), 245-248.
Xiao, J., Porter, S.C., An, Z., Kumai, H. and Yoshikawa, S. (1995) Grain size of quarts as an indicator of winter monsoon strength on the loess Plateau of Central China during the last 130,000 yr: *Quat. Res.*, **43**, 22-29.
Zielinski, U. and Gersonde, R. (1997) Diatom distribution in Southern Ocean surface sediments (Atlantic sector): Implications for paleoenvironmental reconstructions: *Palaeogeogr., Palaeoclimatol., Palaeoecol.*, **129**, 213-250.